Inhibition of Fibrillization and Accumulation of Prefibrillar Oligomers in Mixtures of Human and Mouse α-Synuclein†

Jean-Christophe Rochet, Kelly A. Conway, and Peter T. Lansbury, Jr.*

Morris K. Udall Parkinson's Disease Research Center of Excellence, Center for Neurologic Diseases, Brigham and Women's Hospital, and Department of Neurology, Harvard Medical School, 77 Avenue Louis Pasteur, Boston, Massachusetts 02115

Received June 8, 2000; Revised Manuscript Received July 18, 2000

ABSTRACT: Parkinson's disease (PD) is a neurodegenerative disorder attributed to the loss of dopaminergic neurons from the *substantia nigra*. Some surviving neurons are characterized by cytoplasmic Lewy bodies, which contain fibrillar α-synuclein. Two mutants of human α-synuclein (A53T and A30P) have been linked to early-onset, familial PD. Oligomeric forms of these mutants accumulate more rapidly and/or persist for longer periods of time than oligomeric, human wild-type α-synuclein (WT), suggesting a link between oligomerization and cell death. The amino acid sequences of the mouse protein and WT differ at seven positions. Mouse α-synuclein, like A53T, contains a threonine residue at position 53. We have assessed the conformational properties and fibrillogenicity of the murine protein. Like WT and the two PD mutants, mouse α-synuclein adopts a "natively unfolded" or disordered structure. However, at elevated concentrations, the mouse protein forms amyloid fibrils more rapidly than WT, A53T, or A30P. The fibrillization of mouse α-synuclein is slowed by WT and A53T. Inhibition of fibrillization leads to the accumulation of nonfibrillar, potentially toxic oligomers. The results are relevant to the interpretation of the phenotypes of transgenic animal models of PD and suggest a novel approach for testing the cause and effect relationship between fibrillization and neurodegeneration.

Parkinson's disease (PD)[1] is a neurodegenerative disorder characterized by difficulty in initiating movements, rigidity, and resting tremor (*1*). These symptoms are attributed to the progressive loss of dopaminergic neurons from the *substantia nigra* region of the brain. Some surviving nigral dopaminergic neurons contain fibrous, cytosolic inclusions named Lewy bodies (*2*).

Several observations have implicated the presynaptic protein α-synuclein in the pathogenesis of PD. First, α-synuclein has been shown to be a major fibrillar component of Lewy bodies (*3*−*5*). Second, two mutants of α-synuclein, A53T (*6*, *7*) and A30P (*8*), have been linked to familial PD, a rare early-onset form of the disease that is inherited in an autosomal dominant manner. Third, the production of WT in transgenic mice (*9*) or of WT, A53T, or A30P in transgenic flies (*10*) leads to motor deficits and neuronal inclusions reminiscent of PD.

α-Synuclein is a small (14 kDa), highly conserved presynaptic protein that is abundant in various regions of the brain (*11*−*15*). The level of synthesis of α-synuclein increases during the early stages of postnatal murine brain development (*16*) and during the critical period for song learning in zebra finch (*15*), suggesting that α-synuclein plays a role in synaptic development, function, and plasticity. Knockout mice that lack the gene for α-synuclein exhibit a subtle phenotype that implies that the protein can act as a negative regulator of dopamine release (*17*).

The amino acid sequence of α-synuclein can be divided into N- and C-terminal regions (Figure 1A). The N-terminal region (residues 1−95) consists of seven degenerate, 11-residue repeats, six of which contain the highly conserved hexamer motif KTK(E/Q)GV. The C-terminal region (residues 96−140) is enriched in aspartate, glutamate, and proline. In isolation, α-synuclein adopts an ensemble of unstructured conformations, termed "natively unfolded" (*18*). In contrast, in solutions containing fluorinated alcohols or detergent micelles (*18*), or in the presence of small unilamellar vesicles (*19*), α-synuclein adopts a mostly α-helical structure.

The conformational properties of monomeric WT, A53T, and A30P are similar (*18*, *20*). At high concentrations, all three variants form amyloid fibrils that resemble those in Lewy bodies of PD (*20*−*24*). The fibrils formed in vitro have the features of "amyloid", including staining with amyloid-specific dyes, a prominent β-sheet structure, and a characteristic morphology and size (*23*, *24*). Fibrillization occurs via a nucleation-dependent mechanism (*25*, *26*). The lag time that precedes the appearance of fibrils is shorter for A53T, but longer for A30P, than for WT; therefore, accelerated fibrillization is *not* a shared property of both PD mutants (*20*, *26*). However, A53T and A30P both undergo more rapid oligomerization (defined as the formation of fibrillar *and/or*

† This work was funded in part by grants from the National Institutes of Health (AG08470 and AG14366) and a Zenith Award from the Alzheimer's Association. J.-C.R. was supported by fellowships from the Alberta Heritage Foundation for Medical Research and the Human Frontier Science Program.

* To whom correspondence should be addressed. Telephone: (617) 525-5260. Fax: (617) 525-5252. E-mail: lansbury@cnd.bwh.harvard.edu.

[1] Abbreviations: PD, Parkinson's disease; HFIP, 1,1,1,3,3,3-hexafluoro-2-propanol; SDS, sodium dodecyl sulfate; Aβ, amyloid β-peptide; FTIR, Fourier transform infrared; AFM, atomic force microscopy; EM, electron microscopy; WT, human wild-type α-synuclein; A53T, human A53T α-synuclein; A30P, human A30P α-synuclein.

10.1021/bi001315u CCC: $19.00
Published on Web 08/10/2000

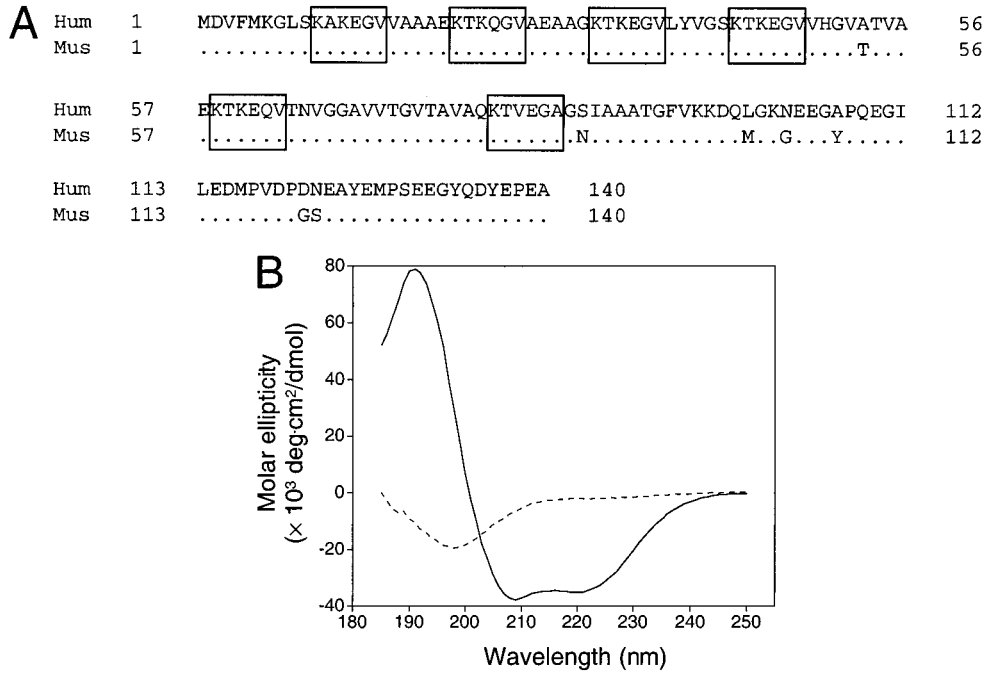

FIGURE 1: Human and mouse α-synuclein have similar primary and secondary structures. (A) Amino acid sequence alignment of WT [Hum (*12*)] and mouse α-synuclein [Mus (*29*)]. Conserved residues of mouse α-synuclein are represented by dots. The six repeats of the hexamer motif KTK(E/Q)GV are boxed. (B) Far-UV CD spectra of the monomeric murine protein in the absence (dashed line) or presence (solid line) of 4% (v/v) HFIP.

nonfibrillar assemblies) than WT (*20*, *22*, *26*). Thus, nonfibrillar oligomers of α-synuclein, rather than the fibrils, may be the toxic species associated with PD (*26*−*28*). Nonfibrillar oligomers of α-synuclein that have been observed by atomic force microscopy include spherical species, chainlike protofibrils, and rings (*20*, *23*, *26*).

Two mouse α-synuclein cDNAs, which encode identical amino acid sequences except at position 58, were isolated independently (*16*, *29*). The sequence of recombinant mouse α-synuclein used in our studies (*29*) differs from the human sequence at seven positions (Figure 1A). One of these differences is at position 53, where the mouse protein contains a threonine residue. Therefore, the A53T mutation is in fact a "reversion" to a residue found in a lower organism, which raises the question of why neither Parkinsonian symptoms nor Lewy bodies have been observed in aged mice. The brains of α-synuclein transgenic mice contain nonfibrillar inclusions of WT that correlate with the degeneration of dopaminergic nerve terminals and the demonstration of motor deficits (*9*). Importantly, the rate of amyloid fibril formation in the brains of the transgenic mice may depend on the ratio of WT to endogenous mouse α-synuclein, which, in turn, most likely varies among different classes of neurons.

To predict the consequences of coproducing the murine and human proteins in the brains of transgenic mice, we have investigated the rate of fibrillization of mouse α-synuclein in the presence and absence of WT or A53T. We demonstrate here that the murine protein (similar to WT) is natively unfolded and forms amyloid fibrils more rapidly than WT or A53T. The fibrillization of mouse α-synuclein is inhibited by WT and A53T. Strikingly, inhibition results in the accumulation of prefibrillar oligomers of α-synuclein (protofibrils). The results of our in vitro studies have implications for interpreting the phenotypes of animal models of PD and suggest a novel strategy for testing the relationship between α-synuclein fibrils, protofibrils, and PD pathogenesis (*28*).

EXPERIMENTAL PROCEDURES

Purification of Recombinant α-Synuclein. Recombinant proteins were produced in *Escherichia coli* and purified as described previously (*23*). One of three expression vectors was used for each protein: pRK172 (provided by R. Jakes and M. Goedert, MRC Cambridge), pET (purchased from Stratagene), and pT7-7 (provided by S. Tabor, Harvard Medical School). The sequences of all DNA constructs were verified by ABI 377 fluorescent DNA sequencing, and the amino acid composition of the pure proteins was confirmed by amino acid analysis.

Preparation of α-Synuclein Solutions for Fibrillization Studies. Purified, lyophilized α-synuclein was dissolved in phosphate-buffered saline (PBS) [0.01 M phosphate buffer, 0.0027 M KCl, and 0.137 M NaCl (pH 7.4)] with 0.02% NaN_3, dialyzed against the same buffer (24 h at 4 °C), and filtered through a Microcon-100 spin filter (MWCO of 1.0 × 10^5 Da), yielding a stock solution that was free of high-molecular mass aggregates (*23*, *26*). Homogeneous samples or mixtures of α-synuclein were prepared by diluting the appropriate stock solutions with buffer (final total protein concentration of 50−600 μM, based on quantitative amino acid analysis) and incubated at 37 °C without agitation. In each experiment, all of the samples were treated identically and in parallel to ensure internal consistency of the data.

Far-UV Circular Dichroism Spectroscopy (CD). Far-UV CD spectra of monomeric and fibrillar mouse α-synuclein (final concentration of 2−7 μM) were collected at 22 °C using an Aviv 62A DS spectropolarimeter and a 0.1 cm cuvette. The data were acquired at 1 nm intervals, with a response time of 4 s per measurement. The final spectrum

was obtained by calculating the mean of three individual scans and subtracting the background. A sample of monomeric mouse α-synuclein was prepared for CD measurements by elution from a Superdex 200 gel-filtration column in 20 mM potassium phosphate (pH 7.4). A solution of fibrillar mouse α-synuclein (300 μM, incubated for 89 days at 37 °C) was diluted in H_2O and centrifuged (16000*g* for 5 min) to separate the fibrils from the monomer.

Fourier Transform Infrared Spectroscopy (FTIR). FTIR spectra of mouse α-synuclein (300 μM, incubated at 37 °C for 32 days) were recorded using a Perkin-Elmer 1600 series spectrophotometer, as described previously (*23*). Second-derivative spectra (based on bandwidth deconvolution) were generated using Perkin-Elmer software.

Congo Red Binding. The binding of Congo red to fibrils of mouse α-synuclein (300 μM, incubated at 37 °C for 32 days) was assessed using a Hewlett-Packard HP8452A UV/VIS spectrophotometer and a 1 cm glass cuvette, as described previously (*23*).

Thioflavin T (Thio T) Fluorescence Assay for Fibril Formation. Aliquots of the α-synuclein incubations (final protein concentration of 5−10 μM in H_2O) were assayed by Thio T fluorescence as described previously (*26*). Fluorescence measurements were carried out using an Analyst microplate analyzer from LJL Biosystems (excitation at 440 nm, bandwidth of 20 nm; emission at 500 nm, bandwidth of 30 nm). All measurements were corrected by subtracting the background fluorescence.

Atomic Force Microscopy (AFM). AFM analysis of mouse α-synuclein (air-dried samples) was carried out as described previously (*20*, *23*, *26*, *30*). Prior to the analysis, a sample of the murine protein (100 μM) was incubated at 37 °C for 86 days. Images were recorded in tapping mode using a Nanoscope IIIa multimode scanning probe workstation (Digital Instruments, Santa Barbara, CA) equipped with an etched silicon NanoProbe (model FESP, 125 μm cantilever, spring constant of 1−5 N/m, tip radius of 5−10 nm). Scanning parameters were within the following ranges: free oscillation amplitude, 0.55−0.9 V; setpoint, 0.3−0.8 V; drive (tapping) frequency, 60−72 kHz; and scan rate, 1.0 Hz.

Electron Microscopy (EM). EM analysis of mouse α-synuclein (300 μM, incubated at 37 °C for 32 days) was carried out using a JEOL 1200 EX transmission electron microscope, as described previously (*20*, *23*).

Gel-Filtration Separation of Monomeric and Oligomeric α-Synuclein from Fibrils. At various times, a 5 μL aliquot of each α-synuclein incubation was diluted in PBS (final volume of 50 μL) and centrifuged at 16000*g* for 10 min to sediment the fibrils. A 40 μL aliquot of the supernatant was injected onto a Superdex 200 column and eluted in PBS, as described previously (*26*). The eluate was monitored at 215 nm, and the contents of each peak were quantified by calculating the peak area using Millenium software.

RESULTS

Mouse α-Synuclein Adopts a Natively Unfolded Conformation. Monomeric mouse α-synuclein eluted from a Superdex 200 gel-filtration column with the same high mobility as WT, A53T, or A30P, reflecting the elongated shape of the murine protein (*18*). The far-UV CD spectrum of monomeric mouse α-synuclein was characterized by a negative minimum at 198 nm (Figure 1B), which typically reflects a random-coil conformation (*31*). The CD spectrum was unchanged after boiling the protein sample, suggesting that mouse α-synuclein, like WT, A53T, and A30P (*18*, *20*), adopts a random-coil or natively unfolded conformation. Also like WT, A30P, and A53T (*18*, *20*), mouse α-synuclein assumed α-helical structure in aqueous solutions containing HFIP (Figure 1B) or SDS. Conceivably, α-synuclein may undergo similar conformational changes in vivo in response to fluctuations in solvent polarity.

Mouse α-Synuclein Forms Amyloid Fibrils. Solutions of recombinant mouse α-synuclein were filtered to remove high-molecular mass seeds (*23*) and incubated at 37 °C. Within 5−7 weeks, the solutions had become viscous and cloudy, and a "grainy" film was visible on the inner walls of the microcentrifuge tube. Later, the solutions had gel-like properties. These visible changes correlated with a marked increase in Thio T fluorescence (Figure 3). A similar but more rapid transition (complete within days rather than weeks) was observed when samples of mouse α-synuclein were shaken continuously at 37 °C. The maximal absorbance of the amyloid-specific dye Congo red (*32*) was increased and red-shifted in an incubated solution of mouse α-synuclein compared to that of the control buffer. The results suggested that the mouse protein, like WT, A53T, and A30P, forms amyloid fibrils (*23*).

Amyloid fibrils are also characterized by a predominance of β-sheet secondary structure (*33*). An aliquot from an aged sample of the mouse protein was diluted in H_2O, and the fibrils were precipitated by centrifugation. The far-UV CD spectra of the supernatant and resuspended pellet (Figure 2A) reflected a random-coil and β-sheet conformation, respectively (*31*). The FTIR spectrum of a sample of fibrillar mouse α-synuclein contained a high-intensity band at 1628 cm^{-1} and a low-intensity band at 1690 cm^{-1} (Figure 2B). These peaks correspond to a split amide I absorption band that is characteristic of an antiparallel β-sheet structure (*34*). The FTIR spectrum also contained a band at 1665 cm^{-1}, which may reflect α-helix, random coil, and/or β-turn. Both the far-UV CD and FTIR spectra of fibrillar mouse α-synuclein were similar to those of fibrillar WT, A53T, and A30P (*23*).

Fibrils comprising mouse α-synuclein were characterized in greater detail using AFM and EM. Individual fibrils and fibrillar "bundles" (Figure 2C,D) were observed by both methods. The fibrils were straight, rigid, and unbranched, with lengths ranging from 0.1 to 3 μm. Some fibrils apparently consisted of two subfilaments wound around each other via a helical twist (most obvious in Figure 2C, inset). The axial periodicity of the twist was constant within each fibril but varied among different fibrils between 55 and 68 nm (measured by AFM). The mean height to the highest point on the "twisted" fibril, measured by AFM, was 7.6 ± 0.6 nm. The mean fibril diameter determined by EM was 12.1 ± 0.9 nm. The dimensions and morphology of fibrils of mouse α-synuclein were similar to those reported for fibrils of WT, A53T, and A30P (*20*, *23*, *24*) and for amyloid fibrils comprising other proteins (*33*).

Mouse α-Synuclein Fibrillizes More Rapidly Than WT and A53T. Solutions of recombinant mouse α-synuclein, WT, and A53T were incubated at 37 °C and monitored for fibril formation by measuring the Thio T fluorescence (*26*). The initial appearance of fibrillar mouse α-synuclein occurred

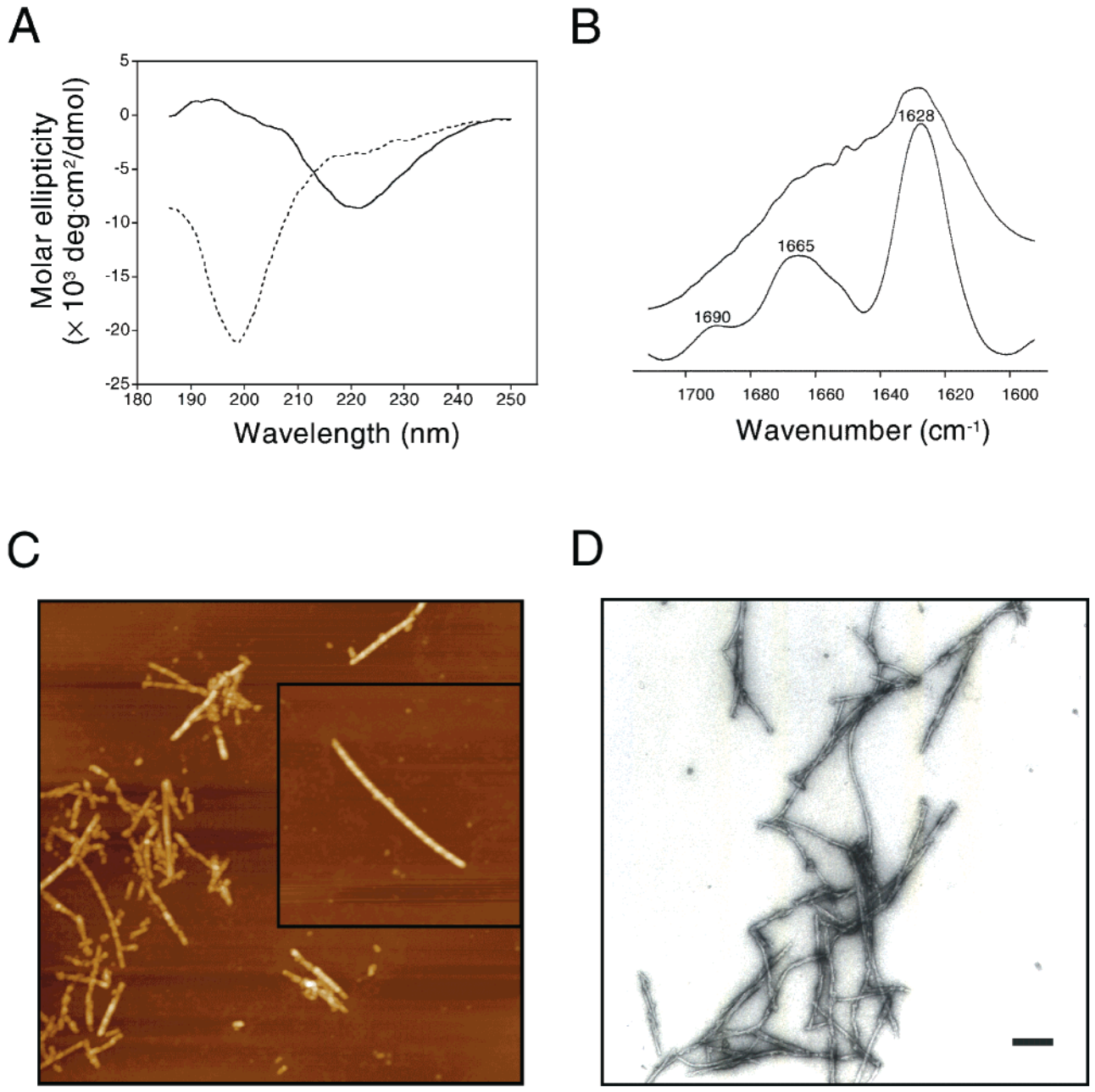

FIGURE 2: Fibrils of mouse α-synuclein have the properties of amyloid. (A) Far-UV CD spectra of the supernatant (dashed line) and resuspended pellet (solid line) obtained by centrifugation of an incubated sample of mouse α-synuclein. (B) Analysis of fibrillar mouse α-synuclein by FTIR spectroscopy. The undeconvoluted and deconvoluted spectra appear at the top and bottom, respectively. (C) AFM images showing fibrils of mouse α-synuclein. Main image, 2 μm × 2 μm; inset image, 1 μm × 1 μm. (D) EM image of fibrillar mouse α-synuclein. Scale bar, 200 nm.

after a lag time (25−30 days) that was shorter than that for WT or A53T (Figure 3A).[2] CD measurements confirmed that the conversion to β-sheet occurred more rapidly for mouse α-synuclein than for WT (results not shown). Monomeric mouse α-synuclein was consumed more rapidly than WT, A53T, or A30P (one experiment shown in Figure 4B). The consumption of the monomeric mouse protein coincided with the formation of fibrils (compare Figures 3B and 4B).

Fibrillization of Mouse α-Synuclein Is Inhibited by WT or A53T. The rate of fibrillization was measured in mixtures of WT and mouse α-synuclein, which are a relevant in vitro model of the total α-synuclein in the brains of transgenic mice. The lag time for fibrillization (Thio T fluorescence) was shorter in a solution of the mouse protein (300 μM) than in an equimolar mixture of WT and mouse α-synuclein (300 μM + 300 μM, 600 μM total) (Figure 3B). By following a more extensive "matrix" of protein samples, in which both the ratio and the total concentration of the mouse and human proteins were varied, we confirmed that fibrillization occurs most rapidly in the most concentrated solutions of pure mouse α-synuclein. Moreover, the lag time in solutions containing a fixed amount of the mouse protein increased with increasing concentrations of WT. For example, after 67 days, the Thio T signal was increased significantly in solutions of ≥150 μM mouse α-synuclein,

[2] The rate of fibrillization of WT was slower than in previously reported experiments (*25*, *26*). This is attributed to important differences in the experimental protocol (for example, the filtration of the samples through a 1.0 × 10^5 Da MWCO filter and the inclusion of sodium azide).

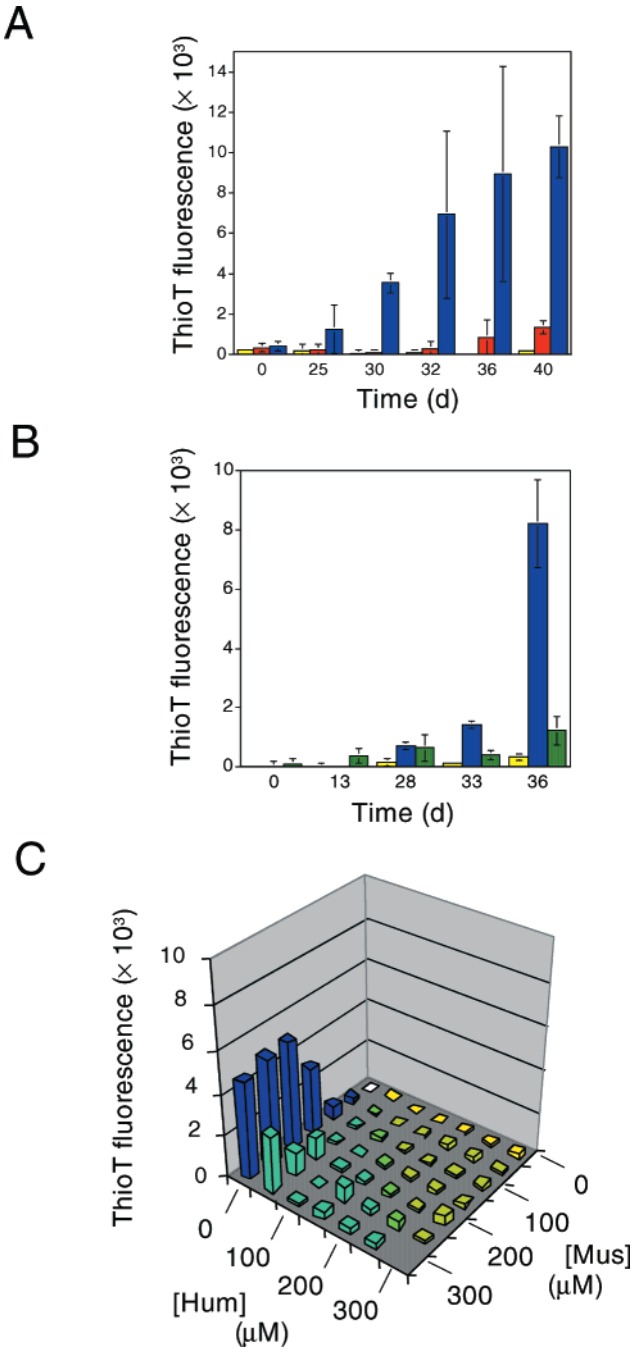

FIGURE 3: Fibrillization of mouse α-synuclein is more rapid than that of WT or A53T and is inhibited in mixtures with WT. (A) Thio T fluorescence in a solution of 300 μM WT (yellow), A53T (red), or mouse α-synuclein (blue). (B) Thio T fluorescence in a solution of WT (300 μM; yellow), mouse α-synuclein (300 μM; blue), or both proteins (300 μM each; green). (C) Thio T fluorescence in a matrix of solutions of mouse α-synuclein and WT (0−300 μM each) after 67 days. The blank is shown in white. Data for homogeneous solutions of mouse α-synuclein and WT are shown in blue and yellow, respectively. Data for mixtures are shown in different shades of green. A solution of 300 μM mouse α-synuclein and 300 μM WT was not analyzed. All incubations were carried out at 37 °C.

while among the mixtures, a significant signal was only detected in the solution containing 300 μM mouse α-synuclein and 50 μM WT (Figure 3C). After 74 days, the magnitude of the signal was increased substantially in all solutions containing only the mouse protein and in mixtures containing mouse α-synuclein (≥150 μM) and WT (≤200

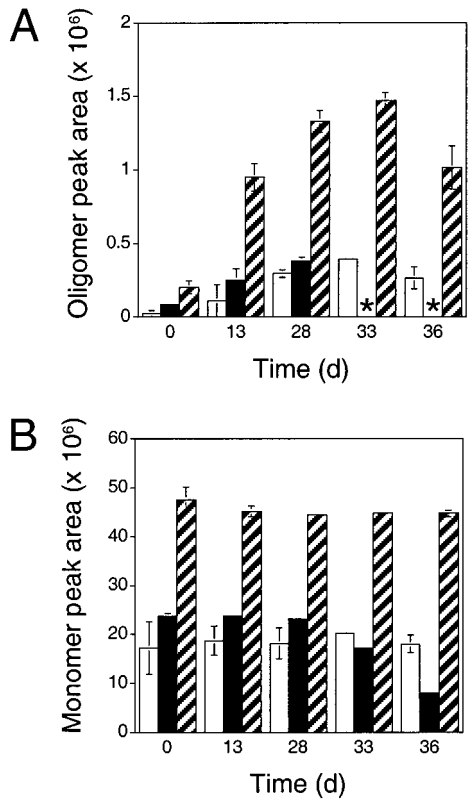

FIGURE 4: Accumulation of nonfibrillar oligomers in mixtures of WT and mouse α-synuclein. The area under the peak corresponding to the oligomer (A) or monomer (B) is shown for a solution of WT (300 μM; white), mouse α-synuclein (300 μM; black), or both proteins (300 μM each; striped), incubated at 37 °C. Asterisks indicate that no oligomer peak was detected.

μM) (results not shown). Again, the magnitude of the signal in the mixtures decreased with increasing concentrations of WT. A significant Thio T signal was first detected in solutions of pure WT (≥250 μM) after 89 days, and its magnitude was increased after 105 days (results not shown). A weaker signal was detected in solutions of WT that also contained relatively low concentrations of the mouse protein. Thus, the fibrillization of WT is inhibited by small amounts of mouse α-synuclein. Finally, we demonstrated a similar inhibitory effect with A53T. Fibrils formed more rapidly (gelation, consumption of monomer) in a solution of mouse α-synuclein (300 μM) than in an equimolar mixture of the mouse protein and A53T (300 μM + 300 μM, 600 μM total) (results not shown).

Nonfibrillar Oligomers Accumulate in Mixtures of Mouse and Human α-Synuclein. The samples monitored for Thio T fluorescence (Figure 3B) were also examined by gel-filtration chromatography, to identify and quantitate pre-fibrillar species of α-synuclein. At the start of the experiment (time zero), each sample contained the monomer and some preformed oligomer, which accounted for ≥97% and ≤0.5% of the total protein, respectively (Figure 4A,B). Upon incubation at 37 °C and prior to the onset of fibrillization, the concentration of the oligomer in each sample increased substantially, with little detectable change (within experimental error)[3] in the amount of monomer. After 33 days, the oligomer was no longer detected in the sample of mouse α-synuclein, and the concentration of the monomer had decreased substantially. In contrast, the concentration of the oligomer in the solution of WT or in the equimolar mixture

of WT and mouse α-synuclein continued to increase, again with little detectable change in the amount of monomer. Importantly, the concentration of the oligomer in the equimolar mixture was greater than the sum of that in the homogeneous solutions of mouse α-synuclein and WT (especially evident after 33 days). After 36 days, the concentration of the oligomer in the solution of WT or in the equimolar mixture of WT and mouse α-synuclein also began to decrease. In general, the nearly complete disappearance of the oligomer and a substantial decrease in the amount of monomer coincided with the onset of fibrillization. Finally, we showed by AFM that the oligomeric fraction consists of spheres, similar to those reported previously (*20*, *23*, *26*).

DISCUSSION

Mouse and Human α-Synuclein Form Amyloid Fibrils That Are Morphologically Indistinguishable. Fibrils of mouse α-synuclein fit the definition of amyloid on the basis of their staining properties (*32*) and extended β-sheet secondary structure (*33*). Similar observations were reported for fibrils of WT, A53T, and A30P (*23*). The β-sheet secondary structure of fibrillar mouse α-synuclein is consistent with the "cross-β" structure suggested by X-ray and electron diffraction analysis of fibrils comprising human, rat, and zebra finch α-synuclein (*24*). Fibrils of the mouse protein also resembled those comprising WT, A53T, or A30P (*20*, *23*, *24*), Aβ40 or Aβ42 (*35*−*38*), and IAPP (*39*−*41*) with respect to height, diameter, and axial periodicity (*33*).

Two observations suggest that the mouse and human proteins undergo fibrillization via similar mechanisms. First, fibrillar mouse and human α-synuclein share the same "twisted" morphology, which implies that both are formed from two wound filaments (*20*, *23*), like fibrillar Aβ40 (*37*). Second, AFM images of fibrillar mouse α-synuclein contain spherical species that are similar to those described for human α-synuclein (*20*, *23*, *26*) and Aβ (*38*, *42*−*45*). Spherical assemblies of mouse and human α-synuclein, which are also detected in the void-volume fraction by gel filtration, accumulate prior to the onset of fibrillization and are subsequently consumed. These spheres may be early fibrillization intermediates that associate in linear fashion to form chainlike protofibrils (*33*).

Mouse α-Synuclein Is More Fibrillogenic Than the Human Proteins. Mouse α-synuclein underwent nucleation-dependent fibrillization more rapidly than WT or A53T. Serpell et al. (*24*) were unable to distinguish between the rates of fibrillization of A53T and rat α-synuclein, which differs from the mouse protein by a single residue at position 121 (*46*).

The rapid rate of fibrillization of mouse α-synuclein compared to that of A53T suggests that at least one of the six mismatched residues between these two proteins plays a role in fibrillization. Five of these residues are located in the anionic C-terminal region (Figure 1A). Repulsive electrostatic interactions involving the highly charged C-terminal region are thought to contribute to the high kinetic solubility of the WT protein (*18*). Consistent with this prediction, C-terminally truncated mutants of α-synuclein (consisting of residues 1−87 or 1−120) form fibrils more rapidly than WT, A53T, or A30P (*24*). Similarly, the increased fibrillogenicity of mouse α-synuclein may be due to the decreased negative charge and polarity in the C-terminal region compared to that of WT. The critical concentration values measured for mouse and human α-synuclein were similar (results not shown), suggesting that the difference in their fibrillization rates is mostly kinetic.

The results of our analyses of the kinetics of fibrillization of mouse and human α-synuclein are relevant to understanding why neither Parkinsonian symptoms nor Lewy bodies have been observed in aged mice. Since the murine protein forms fibrils even more rapidly than the most fibrillogenic human variant, A53T, the apparent absence of PD and Lewy bodies in aged mice cannot be attributed to the relative rates of fibrillization of mouse and human α-synuclein. Instead, other explanations must be considered. For example, the concentration of free α-synuclein [not bound to a membrane (*47*, *48*) or cytoplasmic partner (*49*, *50*)] may be lower in mice than in humans. Alternatively, the short lifespan of mice (approximately 2 years) may preclude the formation of fibrillar inclusions by mouse α-synuclein.

Fibrillization Is Inhibited in Mixtures of the Mouse and Human Proteins. The fibrillization of mouse α-synuclein occurred after a longer lag time in the presence than in the absence of WT. However, after the onset of fibrillization, the magnitude of the Thio T signal increased with similar rates in the equimolar mixtures and in the corresponding homogeneous protein solutions. The results suggested that a nonproductive interaction between mouse and human α-synuclein inhibits the formation of nuclei rather than the growth of preassembled fibrils. Similarly, Hasegawa et al. (*51*) reported that Aβ40 and Aβ42 are mutually inhibitory with respect to nucleation but not fibril elongation. In addition, the nucleation of hemoglobin polymerization in sickle cell disease is inhibited by increasing the ratio of nonfibrillogenic γ-chains to fibrillogenic, mutant β-chains (*52*). Since the inhibition in mixtures of mouse and human α-synuclein led to the accumulation of prefibrillar "spheres", we infer that oligomers are formed prior to the most highly cooperative step of the α-synuclein fibrillization pathway. In support of this hypothesis, the transition from protofibrils to fibrils of Aβ40 has been shown to be nucleation-dependent (*37*).

The fibrillization of mouse α-synuclein was also inhibited by A53T. This result suggests that the nonproductive interaction between mouse and human α-synuclein is due in part to amino acid sequence mismatches other than that at position 53, in the C-terminal region. Consistent with this hypothesis, preliminary results (not shown) suggest that there is no strong inhibitory effect in mixtures containing two of the three human variants, all of which have identical C-terminal sequences.

Inhibition of Fibrillization in α-Synuclein Mixtures Is Relevant to the Interpretation of Transgenic Animal Phenotypes. An important goal in the field of PD research is to generate an animal model that duplicates the essential features of the disease. Efforts have been directed toward generating transgenic mice that produce human α-synuclein (as well as the endogenous mouse protein), with the

[3] The average relative error in the area under the monomer peak was approximately 6%, while the ratio of the oligomer to monomer never exceeded 3%. Therefore, we were unable to demonstrate a mass balance between the monomer and oligomer.

assumption that an increased steady-state concentration of total α-synuclein in vivo should lead to accelerated Lewy body formation. However, one report states that WT forms *nonfibrillar* inclusions in the brains of transgenic mice (*9*). The failure to observe fibrillar inclusions is consistent with our in vitro results: since fibrillization is slowed in mixtures of mouse and human α-synuclein, we would predict that fibrillar inclusions may not form readily in transgenic mice.

In contrast, fibril formation should be accelerated in animal models that produce a single form of α-synuclein. In support of this hypothesis, the expression of a transgene encoding WT, A53T, or A30P in *Drosophila melanogaster* (which lacks endogenous α-synuclein) leads to the accumulation of fibrillar inclusions in the brain, associated with the degeneration of dopaminergic neurons and the premature loss of locomotor ability (*10*). By analogy to the fly model, we predict that fibrillar Lewy bodies would accumulate more rapidly in the brains of mice that produce WT, A53T, or A30P in the *absence* of the endogenous mouse protein.

The Inhibition of Fibrillization in α-Synuclein Mixtures Suggests a Novel Approach for Identifying the Neurotoxic Species in PD. The correlation between fibrils and amyloid diseases suggests that protein fibrillization is pathogenic (*27*). We have proposed that nonfibrillar oligomers linked to the α-synuclein fibrillization pathway, rather than the end-product fibrils, are associated with PD pathogenesis (*26*, *28*). In support of this hypothesis, protofibrillar α-synuclein has been shown to bind lipid vesicles and increase their permeability (S.-J. Lee et al., manuscript in preparation), suggesting a mechanism by which oligomeric α-synuclein may be toxic in vivo. Moreover, the nonfibrillar inclusions observed in the brains of α-synuclein-transgenic mice were associated with the degeneration of dopaminergic nerve terminals and the development of motor deficits (*9*). These inclusions may represent early intermediates that would eventually coalesce to form fibrils, assuming that the transgenic mice have a sufficiently long lifespan (see above).

It is uncertain whether the Parkinsonian phenotype in α-synuclein-transgenic flies is due to fibrillar or nonfibrillar inclusions, since both types of aggregates were detected in the transgenic fly brain (*10*). To probe whether the fibrils themselves are responsible for pathogenesis, mouse α-synuclein-transgenic flies could be generated. Although fibrils would be expected to form rapidly in the brains of these flies, this fibrillization would not necessarily be linked with rapid neurodegeneration and/or motor deterioration. On the other hand, if the nonfibrillar assemblies caused neurodegeneration, then any perturbation leading to their accumulation should produce a more severe Parkinsonian phenotype. Given our in vitro results, we propose that this hypothesis can be tested by crossing two flies that carry different α-synuclein transgenes, to generate a fly that produces two α-synuclein variants simultaneously. Such a "double" transgenic fly may contain more nonfibrillar aggregates and fewer fibrillar inclusions. However, if the toxic protofibril hypothesis (*28*) is correct, then the neuronal degeneration and motor deficits may be more severe in the double transgenic fly than in either single transgenic parent. The results of this in vivo experiment would provide insight into the pathogenesis of amyloid diseases in general.

ACKNOWLEDGMENT

We thank Michael Volles and Matthew Goldberg for preparing the mouse α-synuclein cDNA, Tomas Ding for advice with the AFM, Seung-Jae Lee for assistance with the gel-filtration chromatography, Richard Nowak for assistance with the protein purification, and Margaret Condron for the amino acid analysis.

REFERENCES

1. Dunnett, S. B., and Bjorklund, A. (1999) *Nature 399* (Suppl.), A32−A39.
2. Forno, L. S. (1996) *J. Neuropathol. Exp. Neurol. 55*, 259−272.
3. Spillantini, M. G., Schmidt, M. L., Lee, V. M.-Y., Trojanowski, J. Q., Jakes, R., and Goedert, M. (1997) *Nature 388*, 839−840.
4. Baba, M., Nakajo, S., Tu, P.-H., Tomita, T., Nakaya, K., Lee, V. M.-Y., Trojanowski, J. Q., and Iwatsubo, T. (1998) *Am. J. Pathol. 152*, 879−884.
5. Spillantini, M. G., Crowther, R. A., Jakes, R., Hasegawa, M., and Goedert, M. (1998) *Proc. Natl. Acad. Sci. U.S.A. 95*, 6469−6473.
6. Polymeropoulos, M. H., Lavedan, C., Leroy, E., Ide, S. E., Dehejia, A., Dutra, A., Pike, B., Root, H., Rubenstein, J., Boyer, R., Stenroos, E. S., Chandrasekharappa, S., Athanassiadou, A., Papapetropoulos, T., Johnson, W. G., Lazzarini, A. M., Duvoisin, R. C., Di Iorio, G., Golbe, L. I., and Nussbaum, R. L. (1997) *Science 276*, 2045−2047.
7. Papadimitriou, A., Veletza, V., Hadjigeorgiou, G. M., Patrikiou, A., Hirano, M., and Anastasopoulos, I. (1999) *Neurology 52*, 651−654.
8. Kruger, R., Kuhn, W., Muller, T., Woitalla, D., Graeber, M., Kosel, S., Przuntek, H., Epplen, J. T., Schols, L., and Riess, O. (1998) *Nat. Genet. 18*, 106−108.
9. Masliah, E., Rockenstein, E., Veinbergs, I., Mallory, M., Hashimoto, M., Takeda, A., Sagara, Y., Sisk, A., and Mucke, L. (2000) *Science 287*, 1265−1269.
10. Feany, M. B., and Bender, W. W. (2000) *Nature 404*, 394−398.
11. Maroteaux, L., Campanelli, J. T., and Scheller, R. H. (1988) *J. Neurosci. 8*, 2804−2815.
12. Uéda, K., Fukushima, H., Masliah, E., Xia, Y., Iwai, A., Yoshimoto, M., Otero, D. A. C., Kondo, J., Ihara, Y., and Saitoh, T. (1993) *Proc. Natl. Acad. Sci. U.S.A. 90*, 11282−11286.
13. Jakes, R., Spillantini, M. G., and Goedert, M. (1994) *FEBS Lett. 345*, 27−32.
14. Iwai, A., Masliah, E., Yoshimoto, M., Ge, N., Flanagan, L., de Silva, H. A. R., Kittel, A., and Saitoh, T. (1995) *Neuron 14*, 467−475.
15. George, J. M., Jin, H., Woods, W. S., and Clayton, D. F. (1995) *Neuron 15*, 361−372.
16. Hsu, L. J., Mallory, M., Xia, Y., Veinbergs, I., Hashimoto, M., Yoshimoto, M., Thal, L. J., Saitoh, T., and Masliah, E. (1998) *J. Neurochem. 71*, 338−344.
17. Abeliovich, A., Schmitz, Y., Farinas, I., Choi-Lundberg, D., Ho, W. H., Castillo, P. E., Shinsky, N., Verdugo, J. M., Armanini, M., Ryan, A., Hynes, M., Phillips, H., Sulzer, D., and Rosenthal, A. (2000) *Neuron 25*, 239−252.
18. Weinreb, P. H., Zhen, W., Poon, A. W., Conway, K. A., and Lansbury, P. T., Jr. (1996) *Biochemistry 35*, 13709−13715.
19. Davidson, W. S., Jonas, A., Clayton, D. F., and George, J. M. (1998) *J. Biol. Chem. 273*, 9443−9449.
20. Conway, K. A., Harper, J. D., and Lansbury, P. T. (1998) *Nat. Med. 4*, 1318−1320.
21. Giasson, B. I., Uryu, K., Trojanowski, J. Q., and Lee, V. M.-Y. (1999) *J. Biol. Chem. 274*, 7619−7622.
22. Narhi, L., Wood, S. J., Steavenson, S., Jiang, Y., Wu, G. M., Anafi, D., Kaufman, S. A., Martin, F., Sitney, K., Denis, P.,

Louis, J.-C., Wypych, J., Biere, A. L., and Citron, M. (1999) *J. Biol. Chem. 274*, 9843−9846.
23. Conway, K. A., Harper, J. D., and Lansbury, P. T., Jr. (2000) *Biochemistry 39*, 2552−2563.
24. Serpell, L. C., Berriman, J., Jakes, R., Goedert, M., and Crowther, R. A. (2000) *Proc. Natl. Acad. Sci. U.S.A. 97*, 4897−4902.
25. Wood, S. J., Wypych, J., Steavenson, S., Louis, J.-C., Citron, M., and Biere, A. L. (1999) *J. Biol. Chem. 274*, 19509−19512.
26. Conway, K. A., Lee, S.-J., Rochet, J.-C., Ding, T. T., Williamson, R. E., and Lansbury, P. T., Jr. (2000) *Proc. Natl. Acad. Sci. U.S.A. 97*, 571−576.
27. Lansbury, P. T., Jr. (1999) *Proc. Natl. Acad. Sci. U.S.A. 96*, 3342−3344.
28. Goldberg, M. S., and Lansbury, P. T., Jr. (2000) *Nat. Cell Biol. 2*, E115−E119.
29. Hong, L., Ko, H. W., Gwag, B. J., Joe, E., Lee, S., Kim, Y.-T., and Suh, Y.-H. (1998) *Neuroreport 9*, 1239−1243.
30. Ding, T. T., and Harper, J. D. (1999) *Methods Enzymol. 309*, 510−525.
31. Woody, R. W. (1995) *Methods Enzymol. 246*, 34−71.
32. Klunk, W. E., Jacob, R. F., and Mason, R. P. (1999) *Anal. Biochem. 266*, 66−76.
33. Rochet, J.-C., and Lansbury, P. T., Jr. (2000) *Curr. Opin. Struct. Biol. 10*, 60−68.
34. Krimm, S., and Bandekar, J. (1986) *Adv. Protein Chem. 38*, 181−364.
35. Harper, J. D., Wong, S. S., Lieber, C. M., and Lansbury, P. T., Jr. (1997) *Chem. Biol. 4*, 119−125.
36. Walsh, D. M., Lomakin, A., Benedek, G. B., Condron, M. M., and Teplow, D. B. (1997) *J. Biol. Chem. 272*, 22364−22372.
37. Harper, J. D., Lieber, C. M., and Lansbury, P. T., Jr. (1997) *Chem. Biol. 4*, 951−959.
38. Walsh, D. M., Hartley, D. M., Kusumoto, Y., Fezoui, Y., Condron, M. M., Lomakin, A., Benedek, G. B., Selkoe, D. J., and Teplow, D. B. (1999) *J. Biol. Chem. 274*, 25945−25952.
39. Goldsbury, C. S., Cooper, G. J., Goldie, K. N., Muller, S. A., Saafi, E. L., Gruijters, W. T., Misur, M. P., Engel, A., Aebi, U., and Kistler, J. (1997) *J. Struct. Biol. 119*, 17−27.
40. Goldsbury, C., Kistler, J., Aebi, U., Arvinte, T., and Cooper, G. J. S. (1999) *J. Mol. Biol. 285*, 33−39.
41. Kayed, R., Bernhagen, J., Greenfield, N., Sweimeh, K., Brunner, H., Voelter, W., and Kapurniotu, A. (1999) *J. Mol. Biol. 287*, 781−796.
42. Harper, J. D., Wong, S. S., Lieber, C. M., and Lansbury, P. T., Jr. (1999) *Biochemistry 38*, 8972−8980.
43. Nybo, M., Svehag, S.-E., and Nielsen, E. H. (1999) *Scand. J. Immunol. 49*, 219−223.
44. Blackley, H. K. L., Patel, N., Davies, M. C., Roberts, C. J., Tendler, S. J. B., Wilkinson, M. J., and Williams, P. M. (1999) *Exp. Neurol. 158*, 437−443.
45. Huang, T. H., Yang, D. S., Plaskos, N. P., Go, S., Yip, C. M., Fraser, P. E., and Chakrabartty, A. (2000) *J. Mol. Biol. 297*, 73−87.
46. Maroteaux, L., and Scheller, R. H. (1991) *Mol. Brain Res. 11*, 335−343.
47. Jensen, P. H., Nielsen, M. S., Jakes, R., Dotti, C. G., and Goedert, M. (1998) *J. Biol. Chem. 273*, 26292−26294.
48. McLean, P. J., Kawamata, H., Ribich, S., and Hyman, B. T. (2000) *J. Biol. Chem. 275*, 8812−8816.
49. Engelender, S., Kaminsky, Z., Guo, X., Sharp, A. H., Amaravi, R. K., Kleiderlein, J. J., Margolis, R. L., Troncoso, J. C., Lanahan, A. A., Worley, P. F., Dawson, V. L., Dawson, T. M., and Ross, C. A. (1999) *Nat. Genet. 22*, 110−114.
50. Ostrerova, N., Petrucelli, L., Farrer, M., Mehta, N., Choi, P., Hardy, J., and Wolozin, B. (1999) *J. Neurosci. 19*, 5782−5791.
51. Hasegawa, K., Yamaguchi, I., Omata, S., Gejyo, F., and Naiki, H. (1999) *Biochemistry 38*, 15514−15521.
52. Eaton, W. A., and Hofrichter, J. (1995) *Science 268*, 1142−1143.

BI001315U